EPJ D
Atomic, Molecular, Optical and Plasma Physics
EPJ.org
your physics journal

Eur. Phys. J. D (2014) 68: 166 DOI: 10.1140/epjd/e2014-50088-4

Monte Carlo analysis of ionization effects on spatiotemporal electron swarm development

Saša Dujko, Zoran M. Raspopović, Ronald D. White, Toshiaki Makabe and Zoran Lj. Petrović

edp sciences
Società Italiana di Fisica
Springer

Eur. Phys. J. D (2014) 68: 166
DOI: 10.1140/epjd/e2014-50088-4

THE EUROPEAN PHYSICAL JOURNAL D

Regular Article

Monte Carlo analysis of ionization effects on spatiotemporal electron swarm development*

Saša Dujko[1,a], Zoran M. Raspopović[1], Ronald D. White[2], Toshiaki Makabe[3], and Zoran Lj. Petrović[1]

[1] Institute of Physics, University of Belgrade, Pregrevica 118, 11080 Belgrade, Serbia
[2] ARC Centre for Antimatter-Matter Studies, School of Engineering and Physical Sciences, James Cook University, 4810 Townsville, Australia
[3] Department of Electronics and Electrical Engineering, Keio University, 3-14-1 Hiyoshi, Yokohama 223-8522, Japan

Received 31 January 2014 / Received in final form 13 March 2014
Published online 27 June 2014 – © EDP Sciences, Società Italiana di Fisica, Springer-Verlag 2014

Abstract. The explicit impact of ionization dynamics on the non-hydrodynamic spatiotemporal development of electron swarms in gases under the influence of an electric field is considered using a Monte Carlo simulation technique. The existence and decay of spatially periodic structures in the electron energy distribution function and electron density profiles are observed. The sensitivity of the transient and steady-state phases of the development of the electron energy distribution function to post-ionization energy partitioning is studied by comparison of three ionization energy partitioning regimes for the ionization model of Lucas and Saelee.

1 Introduction

Knowledge of the spatiotemporal development of the energy distribution function (EDF) is of intrinsic interest from a fundamental physics viewpoint. Periodic structures in gaseous electronics have been known for the last 150 years [1,2] and are fundamental to the operation and interpretation of the well known Franck-Hertz experiment [3–7] that laid the foundations for quantum mechanics. In recent times such studies have been chiefly motivated by numerous applications of non-equilibrium low-temperature plasmas, particularly in the neighborhood of sources and boundaries [8,9].

The first important steps in kinetic studies of the spatiotemporal development of electrons were made by Goedheer and Meijer [10] and by Mahmoud and Yousfi [11]. While Goedheer and Meijer were concerned with the spatiotemporal description of the electron kinetics in a one-dimensional radio-frequency discharge plasma between plane electrodes, Mahmoud and Yousfi were focused on the spatiotemporal variation of the electron distribution function and the associated swarm parameters under conditions of Townsend discharges. Using a two-term expansion of the EDF in Legendre polynomials, Loffhagen and Winkler solved the Boltzmann equation with the aim of understanding the spatiotemporal relaxation of electrons under the influence of spatially homogeneous electric field in the column-anode plasma of a glow discharge in krypton [12]. The same approach was used by Winkler and co-workers to investigate the spatiotemporal response to a cathode-sided disturbance of electrons in the column-anode region of a glow discharge in neon [13]. The spatiotemporal relaxation of electrons in spatially inhomogeneous column-anode plasma regions of glow discharges in argon between plane electrodes has been analyzed in a combined Boltzmann equation-Monte Carlo study [14,15]. Spatial patterns specific to periodic energy gain (from the field) and loss (due to inelastic collisions) of the drifting electrons have appeared at the cathode side in the profiles of the energy distribution function. Almost identical spatiotemporal patterns of the EDF are observed in this paper indicating that non-local response of the electrons in the progression of the relaxation processes is essentially controlled by the elastic and inelastic collisions which play markedly different roles. The progress of the electron kinetics in spatial and spatiotemporal plasma structures has been reviewed by Winkler et al. [13,16], Dujko et al. [8] and Donko [15].

A separate line of studies perhaps best related to the Holst-Oosterhuis layers of spatial profile of emission [1] has been observed in a number of swarm experiments especially at moderate and high E/n_0. These include studies of excitation profiles both experimental and simulated [17], normalization of the cross sections based on these profiles and real time of flight experiments with spatial observation of emission [18,19].

* Contribution to the Topical Issue "Electron and Positron Induced Processes", edited by Michael Brunger, Radu Campeanu, Masamitsu Hoshino, Oddur Ingólfsson, Paulo Limão-Vieira, Nigel Mason, Yasuyuki Nagashima and Hajime Tanuma.

[a] e-mail: sasha@ipb.ac.rs

Progress towards benchmarking of plasma discharge models [20–24], benchmarking of the charge particle transport modules of such models (kinetic, fluid and Monte Carlo) is provided by the swarm (free diffusion) limit. In this regard, much progress has been made over the last decade and there now exits benchmarks for a variety of conditions found in plasma discharges including for d.c. and a.c. electric and magnetic fields as well as benchmarks for modeling of temporal and spatial nonlocality [13,25–27]. The current work contributes to the latter. This study is part of our ongoing investigations of charged particle transport in neutral gases, focused on the spatiotemporal development of EDF. In previous studies we have focused on the spatial evolution of electron swarms under steady-state Townsend conditions [4,7,8,25], ionization [8,28] and more recently including the impacts of applied magnetic fields [25,27,29–31]. In this study, we focus on the impact of the dynamics of ionization on the spatiotemporal evolution of the electron swarm. More specifically, this study addresses the issue of how the partitioning of energy between the scattered and ejected electrons affects the spatial and temporal evolution of the swarm under the influence of an electric field. Similar fundamental swarm studies have been performed for model [32,33] and real gases [34] under steady-state conditions. Under conditions typical for abnormal glow discharges, it was shown that the different representations of the energy sharing in ionization processes lead to differences in the distribution function and in the macroscopic properties of the electrons [24].

This paper is organized as follows. In Section 2 we briefly outline the Monte Carlo technique for simulating the spatiotemporal swarm evolution including ionization. In Section 3 we present the results of a systematic study of spatiotemporal evolution of the swarm for the ionization model of Lucas and Saelee [35], which is briefly discussed in Section 3.1. In Section 3.2 we consider the dynamics of the ionization on the steady-state (spatially averaged) electron distribution function and associated macroscopic transport coefficients in the hydrodynamic regime. In Section 3.3, we then extend our considerations to non-hydrodynamic conditions and simulate the spatiotemporal evolution of the electron distribution function and associated moments including the electron density. In Section 3.4 we study the impact of initial conditions on spatiotemporal electron swarm development, before drawing conclusions from the present investigation in Section 4.

2 Monte Carlo simulation for spatiotemporal evolution of the swarm

We apply a Monte Carlo simulation code that follows a large number of particles (typically 10^6–10^7) through a neutral gas under the influence of uniform electric field [7,21,29]. The code has been systematically tested and verified [21,36]. At time $t = 0$, electrons are initially released from the origin according to the Maxwellian velocity distribution and it is assumed that the charged-particle swarm develops in an infinite space. We have selected conditions in accordance with some of the standard benchmarks so our results should converge to the accepted benchmark calculations for the benchmark cross sections [8,21].

In order to sample spatially resolved transport parameters under hydrodynamic conditions, we have restricted the space and divided it into cells. Every cell contains 100 spatial points, and these points are used to sample spatial parameters of the electron swarm. The spatially resolved EDF is determined as $f(\varepsilon, x, t) = \Delta N/(N\Delta\varepsilon\Delta x)$, where N is the number of particles between x and $x+\Delta x$ at time t, while ΔN is the number of particles with energy $\varepsilon + \Delta\varepsilon$ in a spatial cell $x + \Delta x$. We note that we have the defined the normalization of the EDF such that:

$$\int f(\varepsilon, x, t)d\varepsilon = \int \frac{\Delta N}{N\Delta\varepsilon\Delta x}d\varepsilon = n(x, t), \tag{1}$$

where $n(x, t)$ is the number density of electrons at a position x at time t. Spatially resolved transport properties are defined through appropriate sampling e.g. the spatially resolved averaged energy is given by:

$$\langle\varepsilon\rangle = \frac{1}{n(x, t)}\int \varepsilon f(\varepsilon, x, t)d\varepsilon. \tag{2}$$

For further details on sampling of spatially resolved MC simulation, the reader is referred to [8] and the treatment of ionization is described in [29].

3 Results and discussion

3.1 The Lucas-Saelee ionization model

In this work we consider the Lucas-Salee ionization model [35]. This model has been extensively investigated with the aim of identifying the importance of treating ionization as a true non-conservative process (rather than just an inelastic process) and to understand the sensitivity of electron transport to the partitioning of the available energy between the scattered and ejected electrons. The details of the benchmark model of Lucas and Saelee are [35]:

$$\begin{aligned}
\sigma_{el}(\varepsilon) &= 4\varepsilon^{-1/2}\ \text{Å}^2 \quad \text{(elastic cross section)}\\
\sigma_{ex}(\varepsilon) &= \begin{cases} 0.1(1-F)(\varepsilon-15.6)\ \text{Å}^2, & \epsilon \geq 15.6\ \text{eV (inelastic)}\\ 0, & \epsilon < 15.6\ \text{eV}\end{cases}\\
\sigma_I(\varepsilon) &= \begin{cases} 0.1F(\varepsilon-15.6)\ \ \text{Å}^2, & \epsilon \geq 15.6\ \text{eV (ionization)}\\ 0, & \epsilon < 15.6\ \text{eV}\end{cases}\\
m/m_0 &= 10^{-3}\\
E/n_0 &= 10\ \text{Td}\\
T_0 &= 0\ \text{K}.
\end{aligned} \tag{3}$$

Here ε is defined in units of eV. Elastic and inelastic scattering is assumed isotropic. The parameter F has been used previously to test the importance of the non-conservative nature of ionization. The conservative case

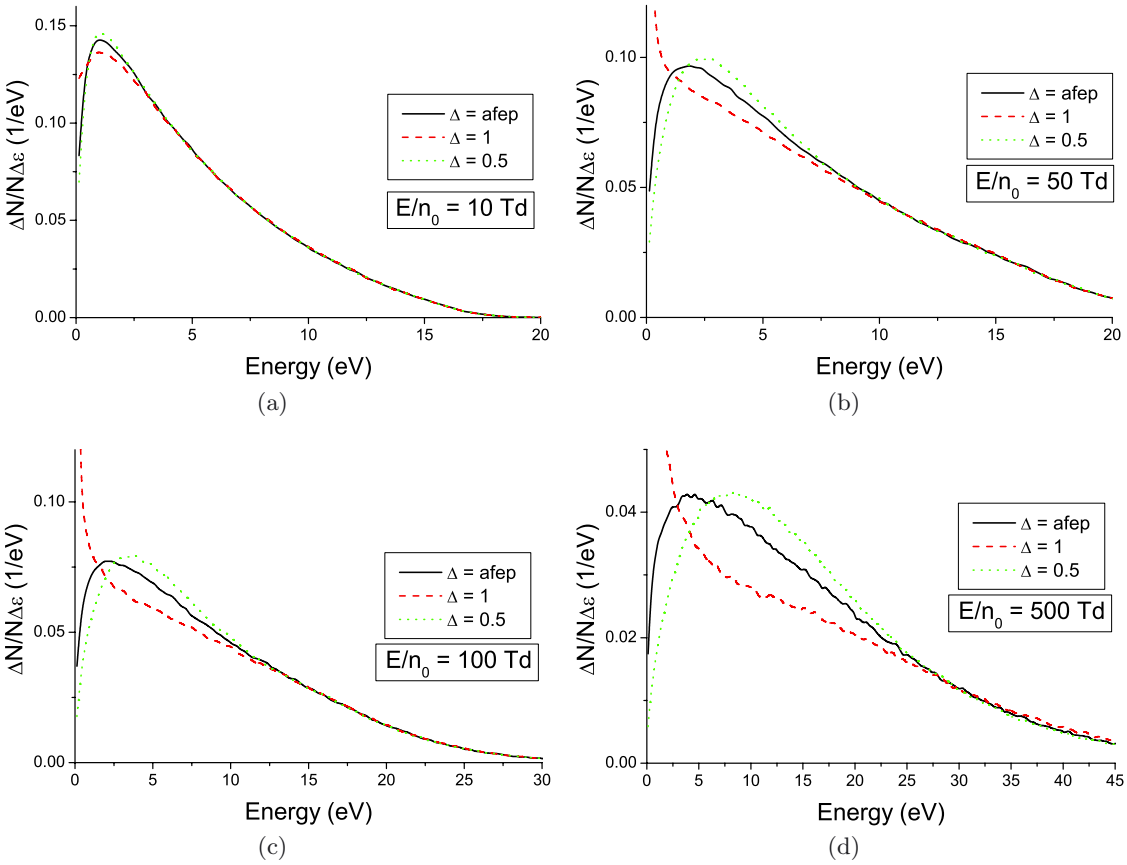

Fig. 1. Impact of the partitioning of energy post ionization on the steady state spatially averaged EDF for electrons in the Lucas-Saelee model for various applied reduced electric fields.

is considered by setting $F = 0$, while the true non-conservative treatment is considered by setting 100% ionization $F = 1$. For ionization our treatment assumes the zeroth order truncation in the mass ratio m/m_0, and we must then define how the available energy is partitioned between the scattered and ejected electrons. We consider three specific cases:

- Δ = afep: all fractions of the distribution of the energy available after the ionization process are equally probable,
- $\Delta = 1$: all energy available after the ionization process is give to either the scattered or ejected electron,
- $\Delta = 0.5$: all energy available after the ionization process is split evenly between the scattered or ejected electrons.

Transport properties are a function of the reduced electric field E/n_0 (where n_0 is the gas number density and is set to 3.54×10^{22} m^{-3}, which corresponds to the pressure of 1 torr at 273 K) which are expressed in units of Townsend (1 Td $= 10^{-21}$ V m^2). Our code has been benchmarked against independent Boltzmann equation solutions under steady state hydrodynamic [36,37], temporally hydrodynamic [38,39] and steady-state Townsend conditions [8,25].

We begin our investigations by understanding the variation of the EDF and associated hydrodynamic transport coefficients in Section 3.2. In Section 3.3 we then focus on the impact of ionization energy partitioning on the non-hydrodynamic evolution of the electron swarm.

3.2 Steady-state spatially-averaged EDF and hydrodynamic transport properties

In this section we consider the variation of the steady state spatially-averaged EDF as a function of applied electric field, and assess the importance of the partitioning of energy post ionization under hydrodynamic conditions. The spatially averaged steady state EDFs are calculated for the three different non-conservative ionization models ($F = 1$) and displayed in Figure 1. At low fields, the fraction of electrons available for ionization is quite low, and consequently the impact of energy partitioning on the distribution function at low fields is quite small. As we increase the field, the fraction of electrons available for ionization is increased and the impact of energy partitioning becomes distinct. For the $\Delta = 1$ case, where all energy goes to one of the electrons while the other has zero energy, the impact on the EDF is quite pronounced through a spike (and maximum) around zero energy. For

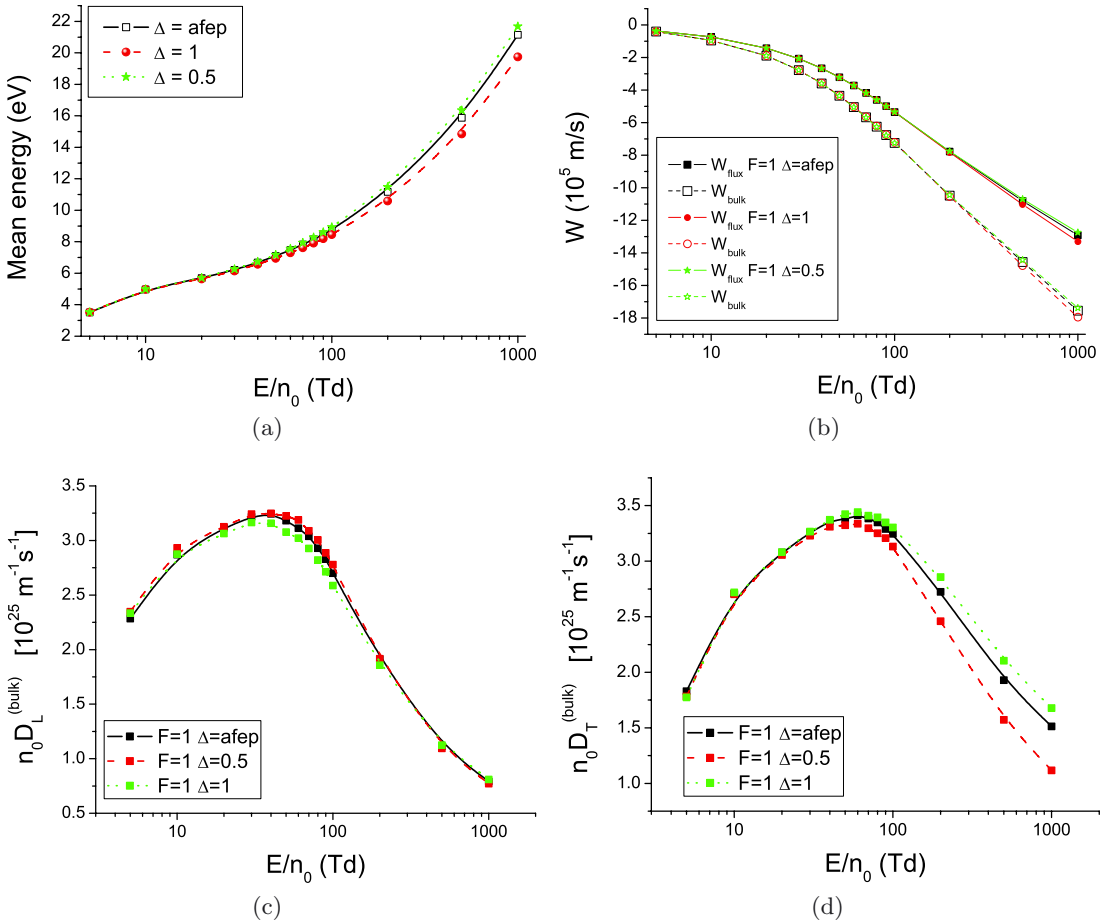

Fig. 2. Impact of the partitioning of energy post ionization on the steady-state hydrodynamic transport properties in the Lucas-Saelee model for various applied reduced electric fields.

the other two-cases $\Delta = 0.5$ and $\Delta =$ afep, the impact is less dramatic. At low fields, the differences between the resulting steady-state EDFs for these two cases are quite small, however as the field increases the differences become more pronounced with the peak in the $\Delta =$ afep distribution appearing at increasingly lower energies relative to the peak in the $\Delta = 0.5$ distribution. For the $\Delta = 0.5$ case, on the average the scattered and ejected electrons will be in the elastic scattering regime allowing an easier increase in their energy. For the $\Delta =$ afep case there is the possibility that some electrons will be scattered/ejected into the inelastic region and be subsequently scattered inelastically to low energies. The differences in the $\Delta = 0.5$ and $\Delta =$ afep distributions then follow. We should emphasize that it is not a result of the number of ionization events – it is not until we get to quite high fields (>100 Td) that there is any appreciable variation in the tail of the distribution and hence ionization rates. The variations in the bulk of the distribution function can however manifest themselves in the macroscopic transport coefficients.

The macroscopic manifestations of the variation of the energy distribution function with the partitioning of the post ionization energy are displayed in Figure 2 where we present the mean energy, bulk and flux drift velocities, as well as the diffusion coefficients parallel $n_0 D_L$ and transverse $n_0 D_T$ to the electric field. The mean energy and flux drift velocity and diffusion coefficients are evaluated as weighted averages over the distribution functions. The bulk coefficients are calculated as spatial averages and the reader is referred to [21] for details of the calculation using MC simulation techniques.

At low fields, transport properties are essentially independent of how the post collision energy is treated due to the low rates of ionization. As we move to higher fields, however, the significant dependencies are increasingly exhibited. For the mean energy, we observe that all $F = 1$ profiles are lower than ionization is treated as an inelastic only $F = 0$. This is well-known ionization cooling that results from the energy sharing between the scattered and ejected electrons. For the $F = 1$ case, the mean energy is always the lowest for the case $\Delta = 1$, while equal sharing $\Delta = 0.5$ produces the highest mean energies. This follows directly from the above discussion of the variations of the EDF with Δ.

The bulk transport coefficients show less sensitivity to how the energy is partitioned after the collision. In addition to the implicit variation associated with the flux quantities, there is an explicit contribution that is

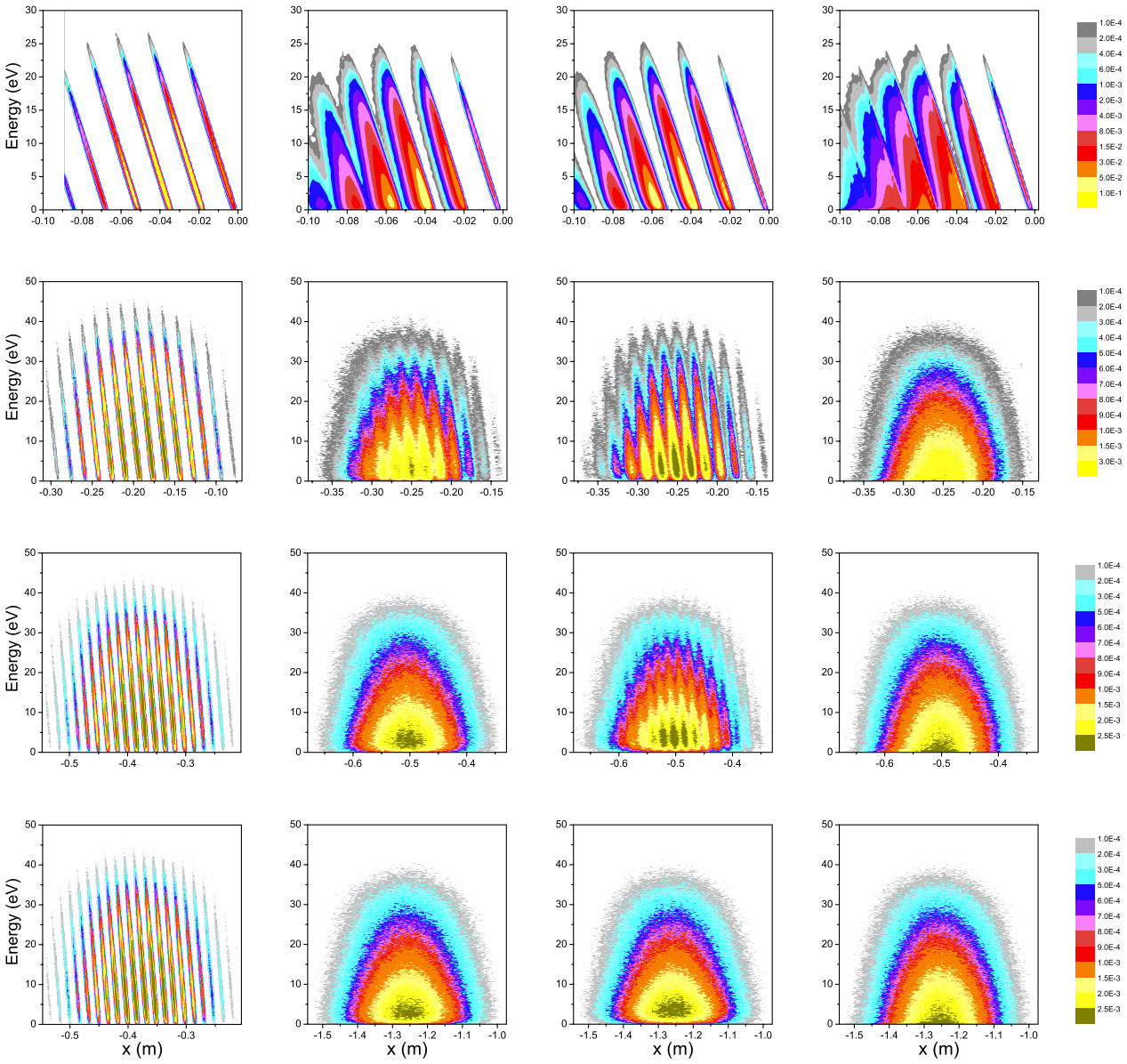

Fig. 3. Spatially resolved EDFs as a function of the ionization parameter F for the instants of time 0.2 μs (first row), 1 μs (second row), and 2 μs (third row) as well as for 5 μs (fourth row). In the first column we show the results for $F = 0$ (conservative case), while in the second, third and fourth columns we show EDFs for random energy partitioning $\Delta =$ afep, equal energy partitioning $\Delta = 0.5$ and zero progeny energy $\Delta = 1$, respectively, within the $F = 1$ (non-conservative case) ionization model.

dependent on how the electrons are generated throughout the swarm. This is related to how the average energy of the electrons vary throughout the swarm, and the variation of the explicit contributions with ionization partitioning appears minimal with the primary impact being on the flux contributions.

3.3 Non-hydrodynamic EDF

In this section we study the transient evolution of the spatially resolved EDF and transport properties. In Figure 3 we display the temporal variation of the spatially resolved EDFs for conservative ($F = 0$) and the three different non-conservative ionization ($F = 1$) models. In Figure 4 we present the temporal evolution of the spatially resolved electron density and average energy (integrals and weighted integrals over energy space) for the same conditions and instants in time. In each case, the electrons at time $t = 0$ are released isotropically from a Maxwellian velocity distribution with an energy spread of 0.1 eV. The electrons are then followed in both configuration and energy spaces under the action of a reduced electric field of 27 Td. While standard Lucas Saelee model uses 10 Td we use 27 Td to enhance the ionization rate and subsequent effects. The electron swarm is released from the origin and as electric field is oriented to the right, the swarm develops to the left. Due to differences

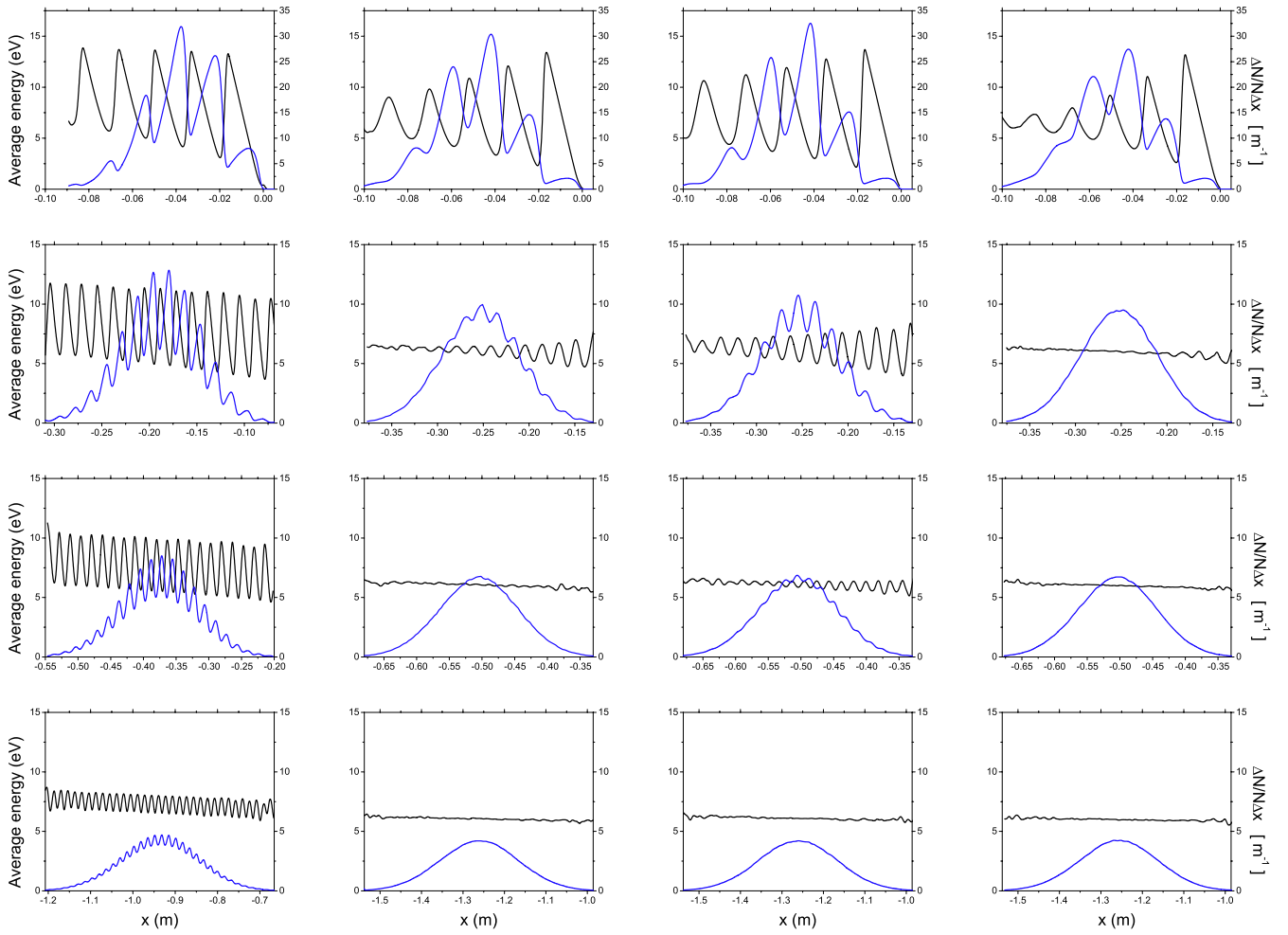

Fig. 4. Spatially resolved average energy (black) and number density (blue) profiles as a function of the ionization parameter F for the instants of time 0.2 μs (first row), 1 μs (second row), and 2 μs (third row) as well as for 5 μs (fourth row). In the first column we show the results for $F = 0$ (conservative case), while in the second, third and fourth columns we show EDFs for random energy partitioning $\Delta =$ afep, equal energy partitioning $\Delta = 0.5$ and zero progeny energy $\Delta = 1$, respectively, within the $F = 1$ (non-conservative case) ionization model.

in the bulk drift velocities between the conservative and non-conservative models (see Fig. 2), the swarms reach different positions in the same time. In what follows, we consider initially the conservative case and then focus on the explicit impact of ionization and the sharing of post-collision energy on their evolution of the EDF.

3.3.1 Conservative case (F = 0): ionization treated as an inelastic process

For the conservative case ($F = 0$) the gas model is reduced to elastic and excitation cross sections and no ionization occurs while for non-conservative case ($F = 1$) the gas model consists of elastic and ionization cross sections and no excitation occurs. In both models the cross sections and thresholds for excitation and ionization have the same magnitude. For the conservative model $F = 0$, we observe that the EDF at any given time is essentially localized to a "pulse" in configuration space, the displacement and width of which increases as time evolves. Interestingly, we note the presence of highly localized beam-like structures in configuration-energy space *within* the EDF pulse. The origin of such structures is quite simple – the acceleration of electrons by the field to higher energies followed by an inelastic collision where the electron loses the threshold energy (the same physics evidenced in the original Franck-Hertz experiment). For a fixed position we observe that the EDF displays localized peaks in the energy space. These localized peaks are similar in shape/width and reflect the assumed initial energy distribution. The energy gap between the peaks in energy space reflects the threshold energy for the inelastic process. Lack of spread of the peaks in energy space reflects the weakness of elastic collisions in this model for exchanging energy. Likewise, for a fixed energy, the EDF displays localized peaks in configuration space. The spatial separation between peaks represents the distance required for the swarm to gain energy from the field equivalent to the threshold energy from the field. The number of spatial oscillations increases in time

reflecting the increase in the width of the "pulse". These spatial oscillations within the pulse exist for long times (much longer than the mean free time between collisions) under conservative conditions due again to the weakness in the elastic collisional processes in this model. This behavior is distinctly non-hydrodynamic. At sufficiently long times, the wavelength of the spatial oscillations is much less than the spatial extent of the EDF and a continuous profile that is essentially Gaussian in configuration space prevails. The swarm has evolved into the hydrodynamic regime.

Integration of the EDF over energy space yields the spatially resolved density profiles shown in Figure 4. At early times we observe spatial structure in the density of electrons within the pulse, the envelope of which is distinctly non-symmetric and non-Gaussian. As the swarm evolves further in time, the amplitude of the spatial oscillations is reduced and the envelope approaches a Gaussian. Eventually (not shown here), these oscillations merge and the standard Gaussian shaped density profile is retained. We also note similar periodic structures in the spatial dependence of the average energy shown in Figure 4. The "saw-tooth" profiles at early times reflect the energy gain from the field followed by inelastic threshold energy loss. The amplitude of the oscillations reduce in both space and time. As expected, the density and average energy oscillation are spatially anti-phase. On spatial locations where the local energy of electrons is minimal, the electrons stay longer comparing to locations where their energy is higher. This situation is a reminisce of the pendulum. The average energy is shown to increase on the average through the swarm in the direction of the drift, consistent with previous studies [40–42].

3.3.2 Non-conservative cases (F = 1): impact of energy partitioning post ionization

When ionization is included explicitly $F = 1$, rather than as an inelastic process $F = 0$ as considered above, we observe in Figure 3 (columns 2 to 4) that EDF has a dramatically different spatiotemporal evolution. Ignoring any differences in the temporal evolution of the spatial envelope of the EDF in the first instance), the beam-like structures in the EDF are significantly modified through the ionization, since the scattered and ejected electrons now populate the low-energy part of the spatially resolved EDF. The distribution of the post-ionization energy to these electrons necessarily modifies where they appear in the EDF and these are reflected in Figure 3 as discussed below.

For early times (see the 0.2 μs profiles), we observe that the first beam in each of the different $F = 1$ EDF profiles are the same as the $F = 0$ profiles, reflecting the absence of ionization for electrons within that beam. Once the ionization processes are operative, we observe an increase in the widths of the EDF beams in configuration and energy space. The EDF transitions from a beam to a spatially periodic structure as electrons travel further from the source and suffer more ionization. The wavelength of the periodic structures are slightly modified from the conservative case, but in general reflect the dominant 15.6 eV threshold energy loss channel (ignoring the elastic energy exchanges which are approximately 3−4 orders of magnitude smaller). When ionization is considered explicitly, the range of energy loss units is no longer fixed. The scattered electron loses energy in units of the threshold plus another loss contribution dependent on how the energy is partitioned post-ionization. The ejected electron appears in a certain part of the EDF dependent on how the post-ionization energy is partitioned. Furthermore, the scattered and ejected electrons now require different distances to reach the threshold energy. Consequently the width of the beams in the EDF are then increased as the swarm evolves in space and time and the periodic beam like structures in the EDF transition to periodic structures and then eventually disappear. Interestingly, the $\Delta = 0.5$ case still preserves its beam-like nature for a longer time than the other partitioning schemes. This is likely a reflection of the equal distances required by the scattered and ejected electrons to reach the threshold energy. At longer times than 5 μs, the EDF and electron density for all ionization models displays no evidence of period structures within the pulse. This contrasts the situation for the inelastic case $F = 0$, where periodic beam-like structures still exist.

In Figure 4 we display the impact of the ionization model on the spatiotemporal evolution of the electron number density. Much of the physics in these plots is detailed in the above discussions of the EDFs. The spatial oscillations in the density profiles are damped out most quickly in the $\Delta = 1$ case. For those cases where spatial oscillations exist in the density profiles, we observe that they have a higher amplitude at the back of the swarm than the front. This is evidence that those at the front of the swarm have undergone more ionization on average than those at the back. Similar amplitude variations through the swarm are observed in the average energy plots and follow from the physics discussed in Section 3.2.

3.4 Impact of initial conditions

To illustrate the impact of initial conditions on the spatiotemporal electron swarm development, in Figure 5 we display the temporal variation of the spatially resolved EDFs for the conservative model ($F = 0$). Calculations are performed assuming the Maxwellian velocity distribution with varying initial mean starting energies ranging from 0 to 10 eV. The beam-like nature of the EDFs for the low mean starting energies have been detailed above. For higher mean starting energies (e.g. for 5 and/or 10 eV), however, the beam like nature is no longer present. The initial energy distributions are broad, and are such that the inelastic channel is essentially now open from the start. The EDF is hence much more spread in configuration-energy space, although the influence of inelastic collisions are clearly visible with the presence of periodic structures

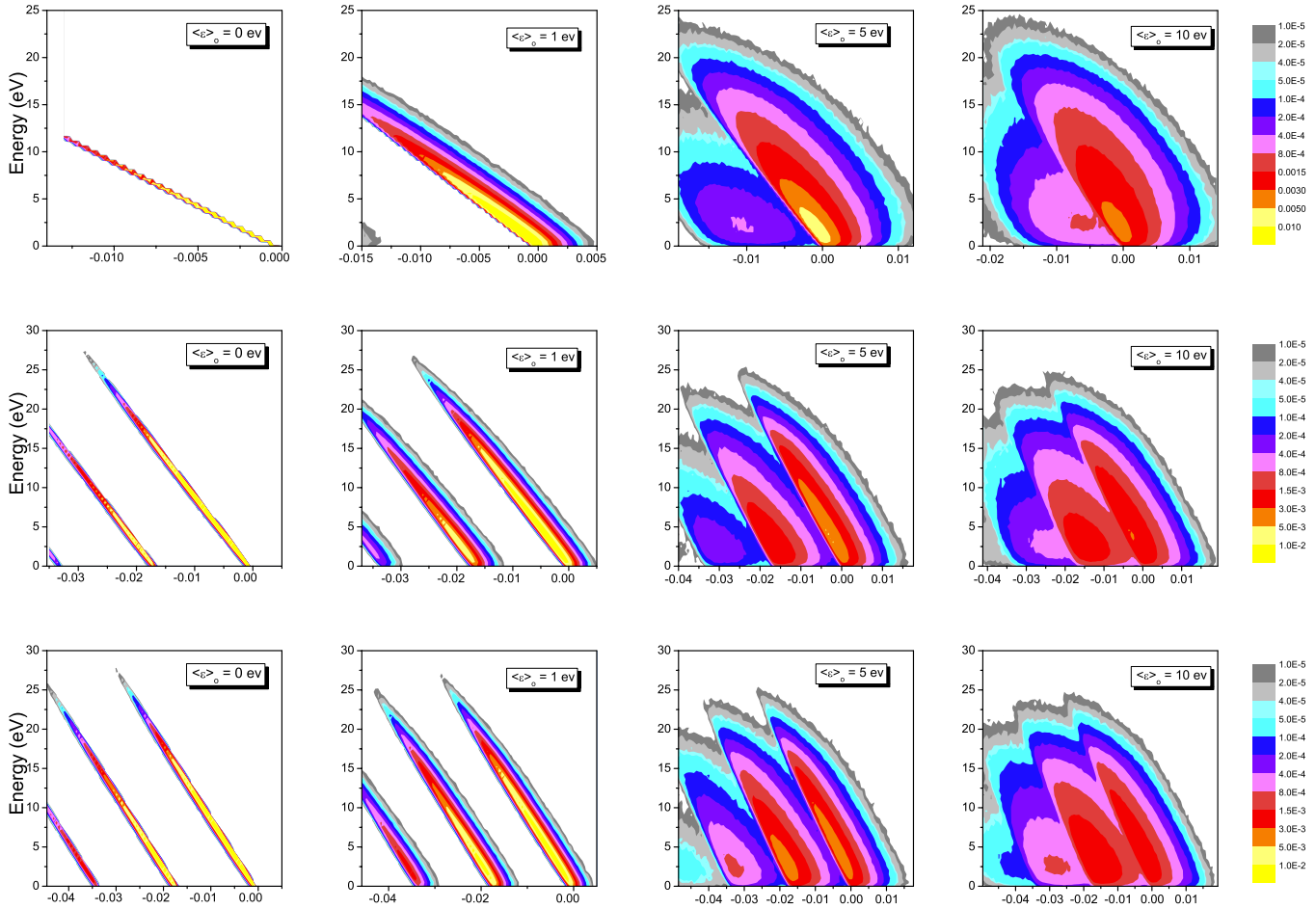

Fig. 5. Spatially resolved EDFs as a function of the mean starting energy for the instants of time 0.1 μs (first row), 0.5 μs (second row), and 0.7 μs (third row). Calculations are performed for the conservative $F = 0$ model. The mean starting energies are indicated in the upper right corner of individual figures. The horizontal axes are x axes and labels are x (m).

in the profiles. These examples clearly demonstrate the influence and importance of the mean initial energy on the spatiotemporal development.

4 Concluding remarks

In this work, we have considered the spatiotemporal evolution of a pulse of electrons in a gas under the action of a spatially homogeneous electric field. The study has shown the existence of transient spatially periodic structures within both the EDF of the electron swarm and the electron density pulse. The decay of these spatially periodic structures was found to be dependent on how the energy is partitioned between the ejected and scattered electrons post-ionization. The study highlights the importance of treating ionization in the correct way (as a non-conservative collisional process rather than as another inelastic process) even for determination of the spatiotemporal evolution of the EDF and associated swarm transport properties.

We should highlight that the spatial structures observed for the model system considered here have been detected in a number of realistic gases [7,12–16,25,29]. The effects of energy-sharing during ionization processes demonstrated in this study will affect the development of these spatiotemporal structures for different conditions for real gases. The presence of numerous inelastic processes present in real gases, which are equally important in the energy balance, would however generally make the effects and spatial structures shown in this study less pronounced.

This work was supported by MNRS Projects ON171037 and III41011, and Australian Research Council.

References

1. G. Holst, E. Oosterhuis, Physica (Amsterdam) **1**, 78 (1921)
2. M.J. Druyvesteyn, Z. Phys. **73**, 33 (1932)
3. J. Franck, G. Hertz, Verh. Deutsche Phys. Ges. **16**, 457 (1914)
4. R.E. Robson, B. Li, R.D. White, J. Phys. B **33**, 507 (2000)
5. F. Sigeneger, R. Winkler, R.E. Robson, Contrib. Plasma Phys. **43**, 178 (2003)

6. P. Magyar, I. Korolov, Z. Donko, Phys. Rev. E **85**, 056409 (2012)
7. R.D. White, R.E. Robson, P. Nicoletopoulos, S. Dujko, Eur. Phys. J. D **66**, 117 (2012)
8. S. Dujko, R.D. White, Z.Lj. Petrović, J. Phys. D **41**, 245205 (2008)
9. P. Nicoletopoulos, R.E. Robson, Phys. Rev. Lett. **100**, 124502 (2008)
10. W.J. Goedheer, P.M. Meijer, J. Nucl. Mater. **200**, 282 (1993)
11. M.O.M. Mahmoud, M. Yousfi, J. Appl. Phys. **81**, 5935 (1997)
12. D. Loffhagen, R. Winkler, J. Phys. D **34**, 1355 (2001)
13. R. Winkler, D. Loffhagen, F. Sigeneger, Appl. Surf. Sci. **192**, 50 (2002)
14. D. Loffhagen, R. Winkler, Z. Donkó, Eur. Phys. J. Appl. Phys. **18**, 189 (2002)
15. Z. Donko, Plasma Sources Sci. Technol. **20**, 024001 (2011)
16. R. Winkler, S. Arndt, D. Loffhagen, F. Sigeneger, D. Uhrlandt, Contrib. Plasma Phys. **44**, 437 (2004)
17. Z.Lj. Petrović, S. Dujko, D. Marić, G. Malović, Ž. Nikitović, O. Šašić, J. Jovanović, V. Stojanović, M. Radmilović-Radjenović, J. Phys. D **42**, 194002 (2009)
18. H.A. Blevin, J. Fletcher, Aust. J. Phys. **45**, 375 (1992)
19. J. Kelly, M.J. Brennan, A.B. Wedding, Aust. J. Phys. **42**, 365 (1989)
20. Z.M. Raspopović, S. Dujko, T. Makabe, Z.Lj. Petrović, Plasma Sources Sci. Technol. **14**, 293 (2005)
21. Z.Lj. Petrović, Z.M. Raspopović, S. Dujko, T. Makabe, Appl. Surf. Sci. **192**, 1 (2002)
22. R.E. Robson, R.D. White, Z.Lj. Petrović, Rev. Mod. Phys. **77**, 1303 (2005)
23. R.D. White, R.E. Robson, S. Dujko, P. Nicoletopoulos, B. Li, J. Phys. D **42**, 194001 (2009)
24. G.K. Grubert, D. Loffhagen, J. Phys. D **47**, 025204 (2014)
25. S. Dujko, R.D. White, Z.Lj. Petrović, R.E. Robson, Plasma Sources Sci. Technol. **20**, 024013 (2011)
26. P. Nicoletopoulos, R.E. Robson, R.D. White, Phys. Rev. E **85**, 046404 (2012)
27. Z.M. Raspopović, S. Dujko, R.D. White, Z.Lj. Petrović, IEEE Trans. Plasma Sci. **39**, 2566 (2011)
28. B. Li, R.D. White, R.E. Robson, J. Phys. D **35**, 2914 (2002)
29. S. Dujko, R.D. White, Z.M. Raspopović, Z.Lj. Petrović, Nucl. Instrum. Methods B **279**, 84 (2012)
30. R.W. Winkler, V.A. Mairov, F. Sigeneger, J. Appl. Phys. **87**, 2708 (2000)
31. B. Li, R.E. Robson, R.D. White, Phys. Rev. E **74**, 026405 (2006)
32. K.F. Ness, R.E. Robson, Phys. Rev. A **34**, 2185 (1986)
33. A.M. Nolan, M.J. Brennan, K.F. Ness, A.B. Wedding, J. Phys. D **30**, 2865 (1997)
34. K.F. Ness, A.M. Nolan, Aust. J. Phys. **53**, 437 (2000)
35. J. Lucas, H. Saelee, J. Phys. D **8**, 640 (1975)
36. Z.M. Raspopović, S. Sakadzić, S. Bzenić, Z.Lj. Petrović, IEEE Trans. Plasma Sci. **27**, 1241 (1999)
37. S. Dujko, R.D. White, Z.Lj. Petrović, R.E. Robson, Phys. Rev. E **81**, 046403 (2010)
38. R.D. White, S. Dujko, K.F. Ness, R.E. Robson, Z. Raspopović, Z.Lj. Petrović, J. Phys. D **41**, 025206 (2008)
39. R.D. White, S. Dujko, R.E. Robson, Z.Lj. Petrović, R.P. McEachran, Plasma Sources Sci. Technol. **19**, 034001 (2010)
40. R.D. White, R.E. Robson, K.F. Ness, Phys. Rev. E **60**, 7457 (1999)
41. K. Maeda, T. Makabe, N. Nakano, S. Bzenić, Z.Lj. Petrović, Phys. Rev. E **55**, 5901 (1997)
42. T. Makabe, Z.Lj. Petrović, *Plasma Electronics: Applications in Microelectronic Device Fabrication* (Taylor and Francis, New York, 2006)